



Surface Technology White Papers

100 (10), 14-22 (November 2013)



2nd Quarterly Report
April-June, 2013
AESF Research Project #R-117

Electrodeposition of Ni-Fe-Mo-W Alloys

by
Prof. E.J. Podlaha-Murphy, Project Director,*
Professor of Chemical Engineering
Northeastern University
Boston, Massachusetts 02115

Editor's Note: This paper was submitted to NASF and AESF Foundation Research Board for the second project quarterly report for AESF Foundation Research Project R-117, April-June, 2013.

Introduction

This NASF-AESF Foundation research project addresses the induced codeposition of molybdenum and tungsten alloys with nickel and iron with a focus on developing a toolbox of plating conditions to deposit different combinations of Ni, Fe, Mo and W. The experimental approach utilizes electrodes with a controlled hydrodynamic environment, since it has been noted by the Project Director that the reduction mechanism can involve a coupled kinetic-mass transport behavior. The project was initiated in January 2013.

This second report follows the work of three students in the lab: undergraduate senior Matthew Silva, graduate student Shaopeng Sun and graduate student Avinash Kola. During the second quarter of the project, we have continued work focused on the effect of electrolyte temperature of NiMoW alloys, the influence of adding Fe(II) to the system, pulse plating of the NiMoW alloys and developing correlations to compare the conventional Hull cell with a rotating Hull cell.

Sub-project #1

Matthew E. Silva, Undergraduate Senior in Chemical Engineering

Mathew Silva started working in our lab last Spring (2013) for course credit and has continued for the summer as a temporary employee. He has surveyed conditions of NiMoW at different electrolyte temperatures over a wide range of current densities employing a rotating Hull cell. From the 1st quarter report, rotating Hull cell (RCH) experiments at 500 rpm were conducted for three average applied current densities (1.0, 2.0 and 3.0 A) and three temperatures (room temperature, 40°C and 60°C). The electrolyte contained 0.15M nickel sulfate, 0.1M sodium tungstate, 0.1M sodium molybdate, 0.375M sodium citrate, and 1.0M boric acid. The pH was adjusted with dilute sulfuric acid or potassium hydroxide to maintain a value of 7.0 ± 0.3 . At an applied average current density of 66.3 mA/cm², there was an effect of temperature on where the deposit formed along the electrode and on the deposit appearance. At lower temperatures, the deposit occurred over a broader distribution, while at higher temperatures, there was an apparent shift in the deposit to the higher current density regions. Figure 1 shows the deposit surface by SEM of two regions on the rotating Hull cell at three temperatures near a high current density region, ~ 120 mA/cm² and a low current density region, ~ 60 mA/cm², where a metallic deposit occurs. At high current densities, nodules are observed which are reduced in size with increasing temperature. At low current densities there is an increase in microcracking with increasing temperature.

*Corresponding author:

Prof. E.J. Podlaha-Murphy
Professor of Chemical Engineering
Northeastern University
Boston, Massachusetts 02115
Phone: (617) 373-3796
E-mail: e.podlaha-murphy@neu.edu

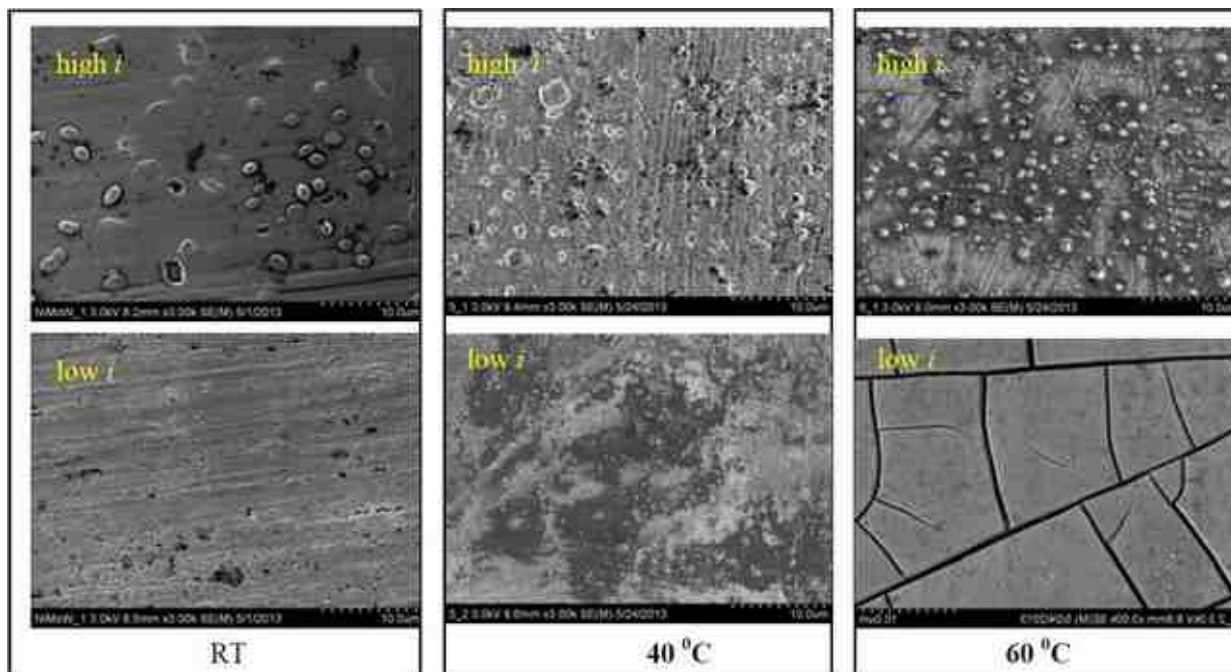


Figure 1 - SEM images of deposits from an electrolyte containing Mo, W and Ni at three different temperatures and two locations on the RHC (low i ~ 60 mA/cm²; high i ~ 120 mA/cm²) at 500 rpm.

The deposit compositions were determined by x-ray fluorescence (XRF), shown in Fig. 2. The x-axis shows where the composition measurement was taken and the span of current density is between ~ 60 and ~ 250 mA/cm². The most unusual observation is that there was no tungsten in the deposit, despite having tungstate in the electrolyte. An increase in temperature, generally led to a lower amount of molybdenum and more nickel in the deposit. Very high amounts of molybdenum were observed, considerably higher than what was generally found in the literature, but at the expense of a very low current efficiency (< 10%).

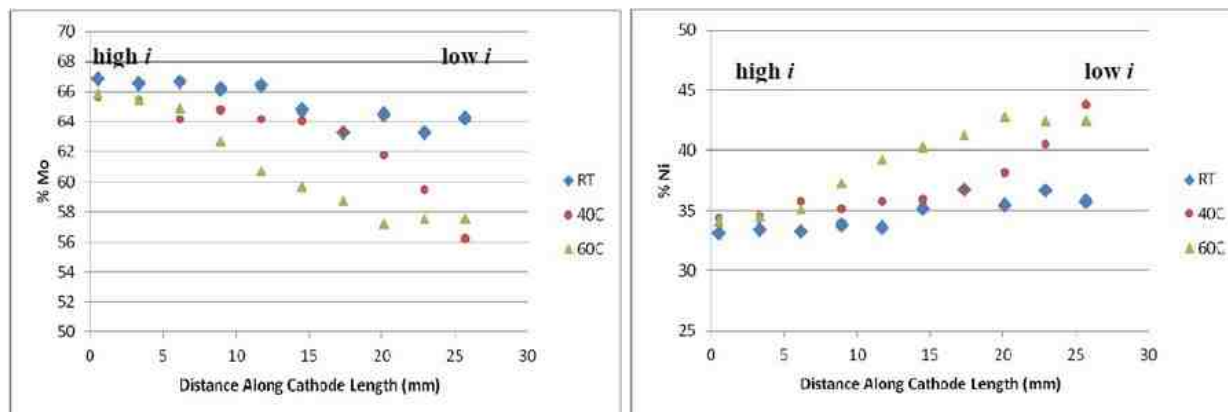


Figure 2 - Deposit wt% molybdenum and nickel on RCH from an electrolyte containing Mo, W and Ni at three different temperatures, 500 rpm, i_{avg} = 66.3 mA/cm²; no tungsten was found in the deposits.

Guided by the RCH results, cylinder experiments at a fixed applied current density, as opposed to a distribution in current, were carried out to verify the current density. Figure 3 shows six samples plated at different current densities, from the Mo, W and Ni electrolyte. Samples 1, 2 and 3 correspond to current densities of 24.75, 33, and 41.25 mA/cm², respectively. Deposits were not "metallic" appearing and did not uniformly cover the brass electrode after a 10-minute deposition. Samples 4, 5 and 6,

corresponding to current densities of 49.5, 66 and 74.25 mA/cm², did appear metallic. The deposit composition of these deposits corresponded to the middle part of the RCH in Fig. 2, showing the consistency of the Hull cell approach.

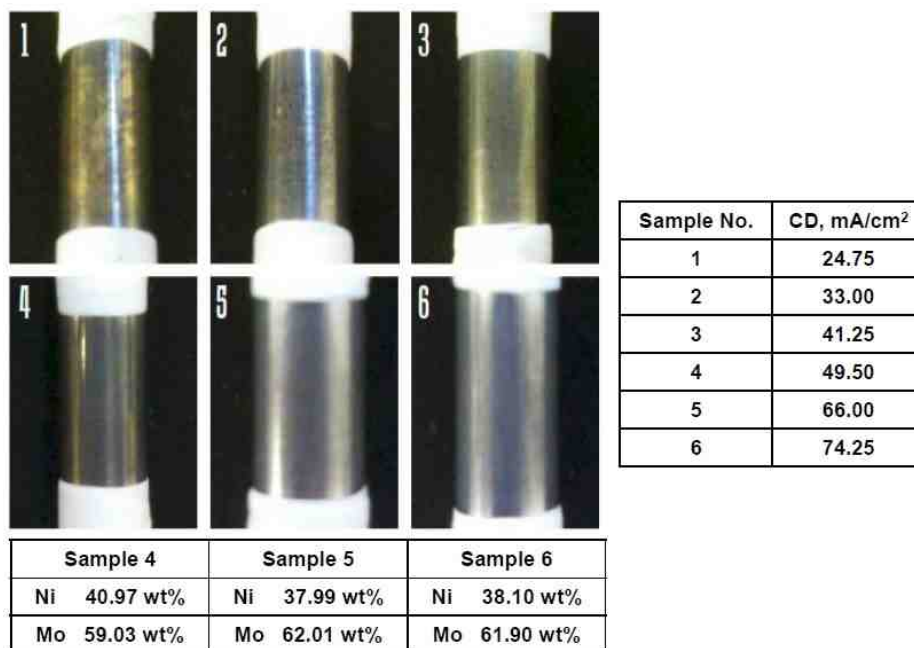


Figure 3 - Rotating cylinder electrodes with deposits from an electrolyte containing Mo, W, and Ni; 500 rpm.

A planned goal of this work has been to explore the effect of adding Fe(II) to the electrolyte. Fe(II) is known to induce the codeposition of both molybdenum and tungsten,¹ but it also can act to reduce the reduction rate of Ni(II).² From a practical point of view, Fe(II) ions can also form Fe(III) at the anode, and thus a two-compartment cell was used for these experiments. Figure 4 shows a schematic of the RHC design. An anodic ion exchange membrane was placed at the bottom of the cathode to separate the anolyte and catholyte.

In addition to the Mo, W and Ni electrolyte, iron sulfate was added at concentrations of 0.15M (equimolar with nickel), 0.10M and 0.05M. Figure 5 show the deposit composition of the resulting Fe-Ni-Mo-W films ranging from high to low current density ranges obtained with the RHC. It was noted that the addition of iron to the Ni-Mo-W electrolyte shows hindrance of nickel and also begins to show codeposition of tungsten at each iron concentration, unlike the electrolyte without the Fe(II). The figures show a marked decrease in nickel content as the iron content increases, with a concomitant drop in the percentage of molybdenum and a slight increase in tungsten content. This is an interesting feature because the data has also shown an inverse relationship as lower iron concentrations lead to higher molybdenum content, which further suggests a preferential coupling of Ni-Mo. As the nickel deposition rate is decreased and its composition goes down in the deposit, so does molybdenum. On the other hand, the iron appears to draw in greater tungsten content.

Figure 6 compares polarization curves of the two electrolytes examined without (a) and with (b) 0.15M Fe(II) at 2.0 mV/sec. When iron is present in the electrolyte, there is an increase in the total current density at potentials more noble than -1.0 V_{SCE}, followed by a maximum and an abrupt decrease in current density where deposition of the alloy occurs. The polarization curves at different temperatures (room temperature, 40°C and 60°C) increase with temperature. The disadvantage of inspecting polarization curves alone is that it is not readily obvious how the individual partial current densities change with temperature and adding Fe(II) to the electrolyte.

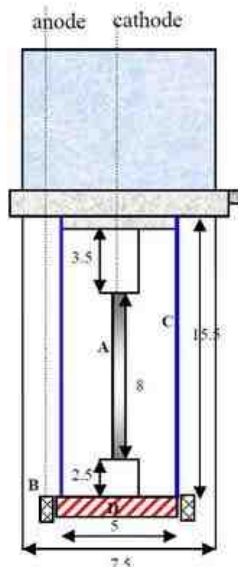


Figure 4 - Schematic diagram of a RHC: (A) electrode, (B) concentric anode, (C) plastic shield placed concentrically around the cylinder cathode and (D) ion exchange membrane (Dimensions in cm).

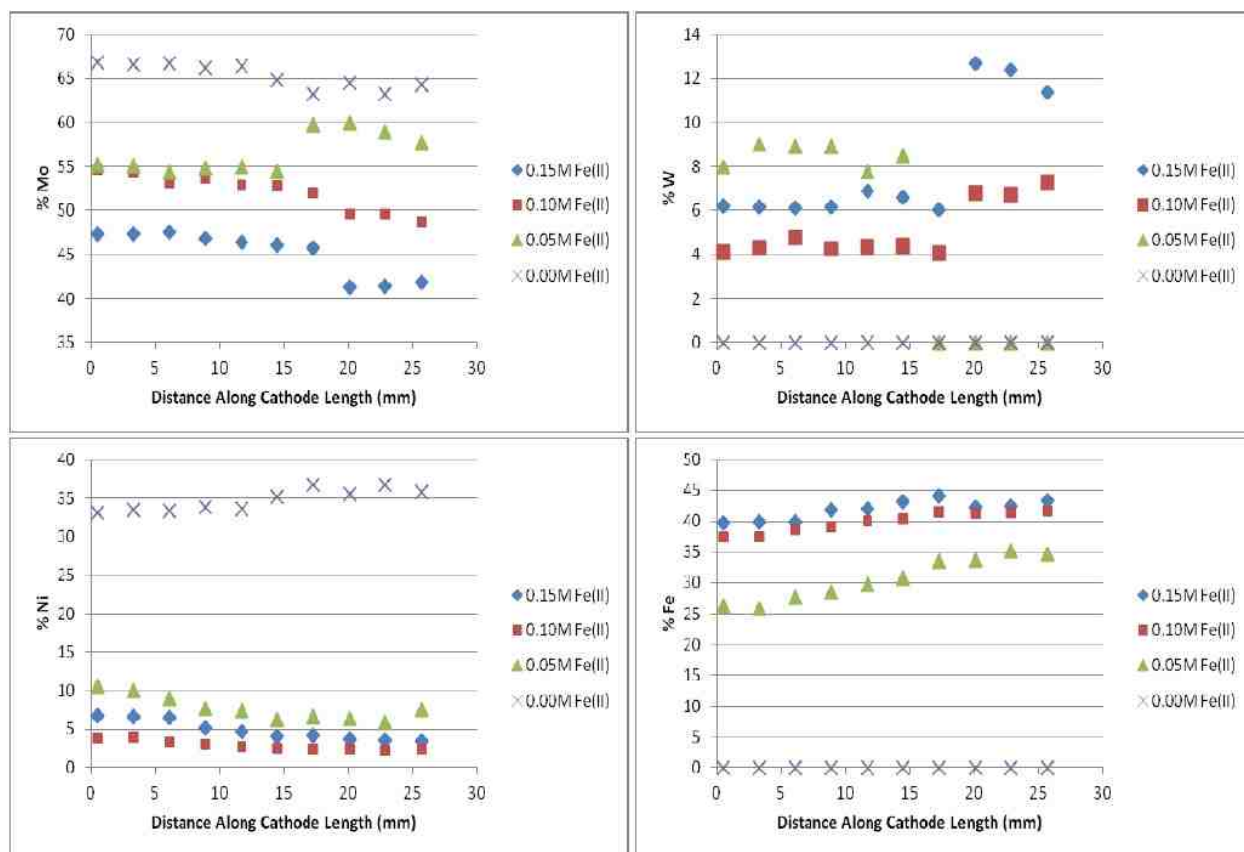


Figure 5 - Fe-Ni-Mo-W deposit composition with variable amounts of Fe(II) added to the electrolyte RHC, 500 rpm, room temperature).

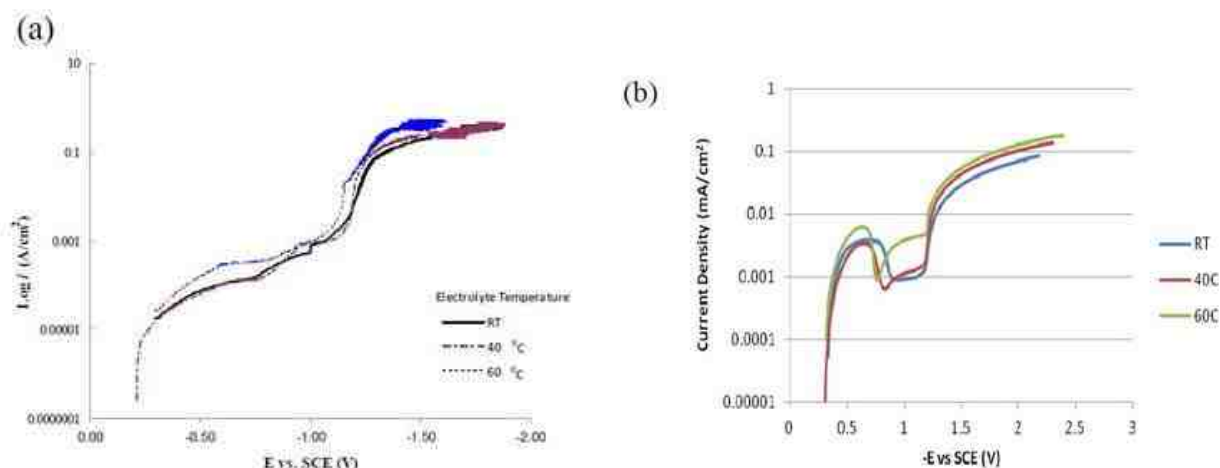


Figure 6 - Polarization curves corrected for ohmic drop at room temperature, 40°C and 60°C; (a) without Fe(II) and (b) when 0.15M Fe(II) is present in the electrolyte. **Note:** Figure 6(a) is reproduced from the 1st quarterly report as a comparison.

Sub-project #2

Shaopeng Sun, Ph.D. graduate student

In the 1st quarterly report, NiMoW alloys were electrodeposited from a different environmentally-friendly electrolyte that yielded all components in the deposit, including tungsten. The electrolyte contained 0.075M sodium tungstate, 0.005M sodium molybdate, 0.1M nickel sulfate, 0.375M sodium citrate and 1.0M boric acid. The pH was adjusted by sodium hydroxide or sulfuric acid to 7.0. No ammonium species were present in the electrolyte. Both pulse deposition and changes of temperature were further examined.

Pulse deposition

To complement the results from our last report, SEM and optical microscopy images were taken of pulsed deposited samples on a rotation cylinder electrode. Figure 7 shows the morphology of NiWMo under pulse current deposition. Optical images of three pulse deposit surfaces are presented. All three deposits have the same on-time per period, 10 msec, with different off-times, having duty cycles of (a) 1/4, (b) 1/2 and (c) 4/5. As seen in Fig. 7, as the duty cycle increases, the cracks in the deposits become more numerous. In other words, the shorter the off-time the more cracks are formed. When the duty cycle is 1/4 [Fig. 3(a)], no observable cracks are present at this scale.

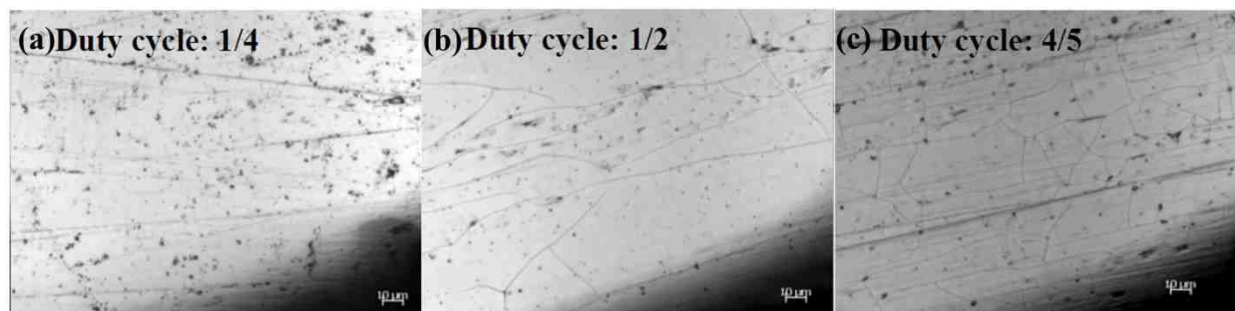


Figure 7 - Optical images of deposits electrodeposited by pulse with duty cycles of (a) 1/4, (b) 1/2 and (c) 4/5 (10 mA/cm^2 pulse current density, 10 msec on-time).

Temperature effect

The electrodeposition temperature effects are presented in Fig. 8. Polarization was performed in the electrodeposition bath at temperatures of 22 (room temperature), 30, 45 and 60°C. The results reflect a higher current density with an increase in temperature. Deposition at different temperatures was conducted with a rotating Hull cell, with an average current density of 20 mA/cm².

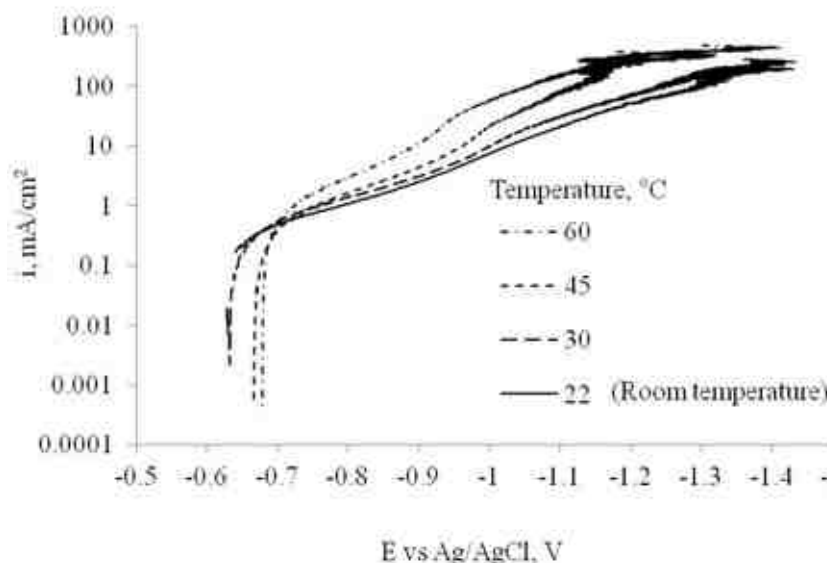


Figure 8 - Polarization at different temperatures conducted with a rotating cylinder electrode (717 rpm, diameter = 0.6 cm).

Figure 9 shows optical photos of the rotating Hull cell samples electrodeposited at varied temperatures. The numbers in white on the sides of the samples are the ratio of local current density to average current density assuming a primary current distribution. It is observed that increased temperature changes the range of electrodeposition. At lower temperatures, a deposit can be obtained when the local current density is less than 20 mA/cm² (where the number in white is 1). However, at a temperature of 60°C, there is no deposit observed until a current density of 40 mA/cm² is reached. At 20 mA/cm² and 30°C and at 45°C, the deposit is silver-like in color, but at 60°C the deposit is an oxide. Table 1 shows the compositions at several points along the electrode. Near the high current density region, the composition does not change significantly with temperature (18-19 wt% Mo, 34-37 wt % Ni, difference W).

The shift in deposition current density observed in Fig. 9 was also observed by Matthew Silva (Sub-project #1) in a similar electrolyte containing NiMoW but with a higher concentration ratio of Ni/(Mo+W) in the electrolyte. In Silva's electrolyte, this ratio was 0.75 and in the electrolyte in this sub-project, the ratio was 1.24. The difference between these two electrolytes is the resulting deposit composition, molybdenum-rich in Silva's case and tungsten-rich in the present case.

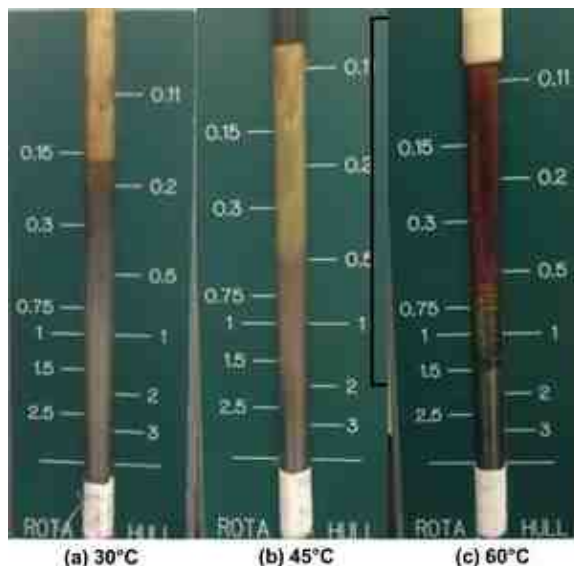


Figure 9 - A comparison of the NiMoW alloy deposit when electrodeposited under DC conditions, at three different temperatures, (a) 30°C, (b) 45°C and (c) 60°C (See also Table 1.).

Table 1 - Compositions of the NiMoW alloy deposits at several points along the electrodes shown in Fig. 9 (DC deposition at (a) 30°C, (b) 45°C and (c) 60°C.).

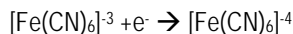
Local current density, mA/cm ²	30°C			45°C			60°C		
	Composition (wt%)								
	Mo	Ni	W	Mo	Ni	W	Mo	Ni	W
20	14	44	42	22	36	42	---	---	---
30	12	43	45	10	42	48	---	---	---
40	15	40	45	14	37	49	---	---	---
50	16	38	46	---	---	---	12	42	46
60	19	34	47	18	34	48	19	37	44

Sub-project #3:

Avinash Kola, starting Ph.D. graduate student.

Characterization of air agitation in a Hull cell

The objective of this characterization is to establish a general relation to estimate the limiting current density of any alloy plating system. For this purpose, a ferricyanide reduction reaction was examined with varying flow rates (air bubbling). A potassium cyanide electrolyte consisting of 0.02M K₃Fe(CN)₆, saturated with 0.5M NaOH was used. The diffusivity of the species was taken as $D = 7.1 \times 10^{-6}$. A ferricyanide reduction is a convenient system, because the reduction happens without undergoing a physical deposition on the surface of the cathode, and thus multiple reactions can be run under different conditions



As shown in Fig. 10(a), a polarization at a scan rate of 5.0 mV/sec was performed to identify the limiting current region with varying flow rates. The limiting current increases with increasing flow rate which is as expected. This limiting current indicates that the reaction is mass transport controlled. An increase in agitation decreases the boundary layer thickness near the cathode surface and hence allows better control over the current distribution.

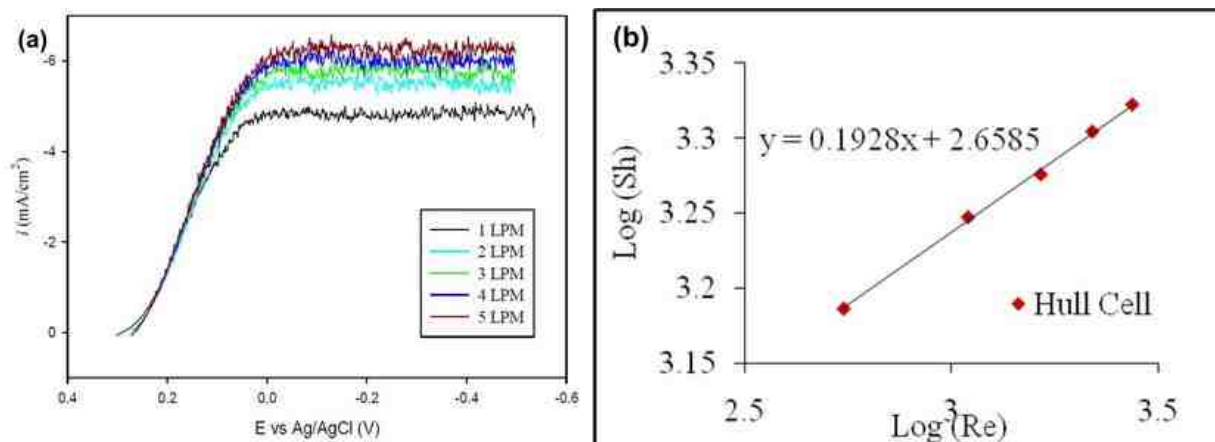


Figure 10 - (a) Polarization curve for ferricyanide reduction with varying flow rates; (b) Plot of $\log SH$ vs $\log Re$ with data obtained from a Hull cell for varying flow rates.

A dimensional analysis for mass transfer by forced convection takes the form through a general correlation, which is a function of dimensionless numbers: Sherwood, Reynolds and Schmidt:

$$Sh = \frac{i_{lim}L}{nFDC^b} = \frac{L}{\delta} \quad (1)$$

$$Re = \frac{\left(\frac{Q}{A}\right)L}{\nu} \quad (2)$$

$$Sc = \frac{\nu}{D} \quad (3)$$

$$\text{or, } Sh = aRe^bSc^{1/3} \quad (4)$$

where a and b are constants, experimentally determined.

The correlation determined from the limiting current values for air bubbling in a convention Hull cell is thus,

$$Sh = 40.6Re^{0.19}Sc^{1/3} \quad (5)$$

In order to replicate the deposition parameters on a rotating cylinder Hull cell, to correlate air bubbling from a conventional Hull cell to a rotation rate for the rotating Hull cell, a correlation is used for a cylinder electrode, Eisenberg equation,

$$Sh = 0.0791Re^{0.7}Sc^{0.356} \quad (6)$$

A comparison between plating an alloy in the Hull cell and RHC is underway.

Dissemination

Two presentations were made thus far of the NASF and AESF Foundation supported work:

1. E.J. Podlaha, A. Kola & S. Sun, "NiWAg, NiWMo and NiW Electrodeposition," SUR-FIN 2013, Rosemont, IL, June 12, 2013 (invited).
2. S. Sun & E.J. Podlaha, "Pulse Electrodeposition of NiMoW Alloys," The 223rd Electrochemical Society (ECS) Meeting, (F2) Toronto, Canada, May 2013.

One proceedings publication resulted from the talk at The Electrochemical Society in May.

Overall summary

The same three students participated in the NASF-AESF Foundation research this quarter as in the start of the project and have made significant progress in each of their respective areas. The large body of work that Matthew Silva has completed presents very interesting results with regard to the effect of iron in the mixed tungsten, molybdenum and nickel electrolytes. The introduction of Fe(II) helps to promote tungsten, and inhibits both nickel and molybdenum. These results will be summarized in a manuscript for publication and will be presented at the 2014 SUR-FIN meeting in Cleveland, Ohio.

The most significant aspect of Sun's results is that pulse deposition has the most dramatic effect in morphology. Longer off-times produce deposits with fewer macro-cracks than shorter ones, attributed to the lowering of adsorbed hydrogen from the side reaction. Overall, the current efficiency is very low, and so efforts to decrease the side reaction by investigating higher electrolyte temperature were initiated. The experiments with the rotating Hull cells showed that there was a shift where deposition occurs to higher current densities with higher temperature.

Kola has targeted a study to investigate the NiW system with thiourea. A correlation was developed to characterize air bubbling.

References

1. A. Brenner, *Electrodeposition of Alloys*, Academic Press, New York. (1963).
2. H. Dahms & I. M. Croll, *J. Electrochem. Soc.*, **112** (8) 771 (1965).

About the authors



Dr. Elizabeth Podlaha-Murphy is a Professor of Chemical Engineering at Northeastern University, Boston, MA. She has been active in electrodeposition for more than 20 years and currently leads efforts in the understanding of reaction mechanisms and kinetic-transport behavior governing electrodeposition. She received her Ph.D. in 1992 from Columbia University, New York, NY and a B.S./M.S. from the University of Connecticut, Storrs, CT.



Matthew Silva is a recent B.S. graduate from the Department of Chemical Engineering, Northeastern University. He completed a co-op position at Xtalic Inc. working in the area of NiW plating. He plans to attend graduate school.



Shaopeng Sun is a senior graduate student in the Department of Chemical Engineering at Northeastern University. He received his B.S. in 2009 from Dalian University of Technology, China.



Avinash Kola is a current graduate student in the Department of Chemical Engineering at Northeastern University. He received his B.S. from Jawaharlal Nehru Technological University, India in 2006 and a M.S. from Louisiana Tech, Ruston, LA in 2010.